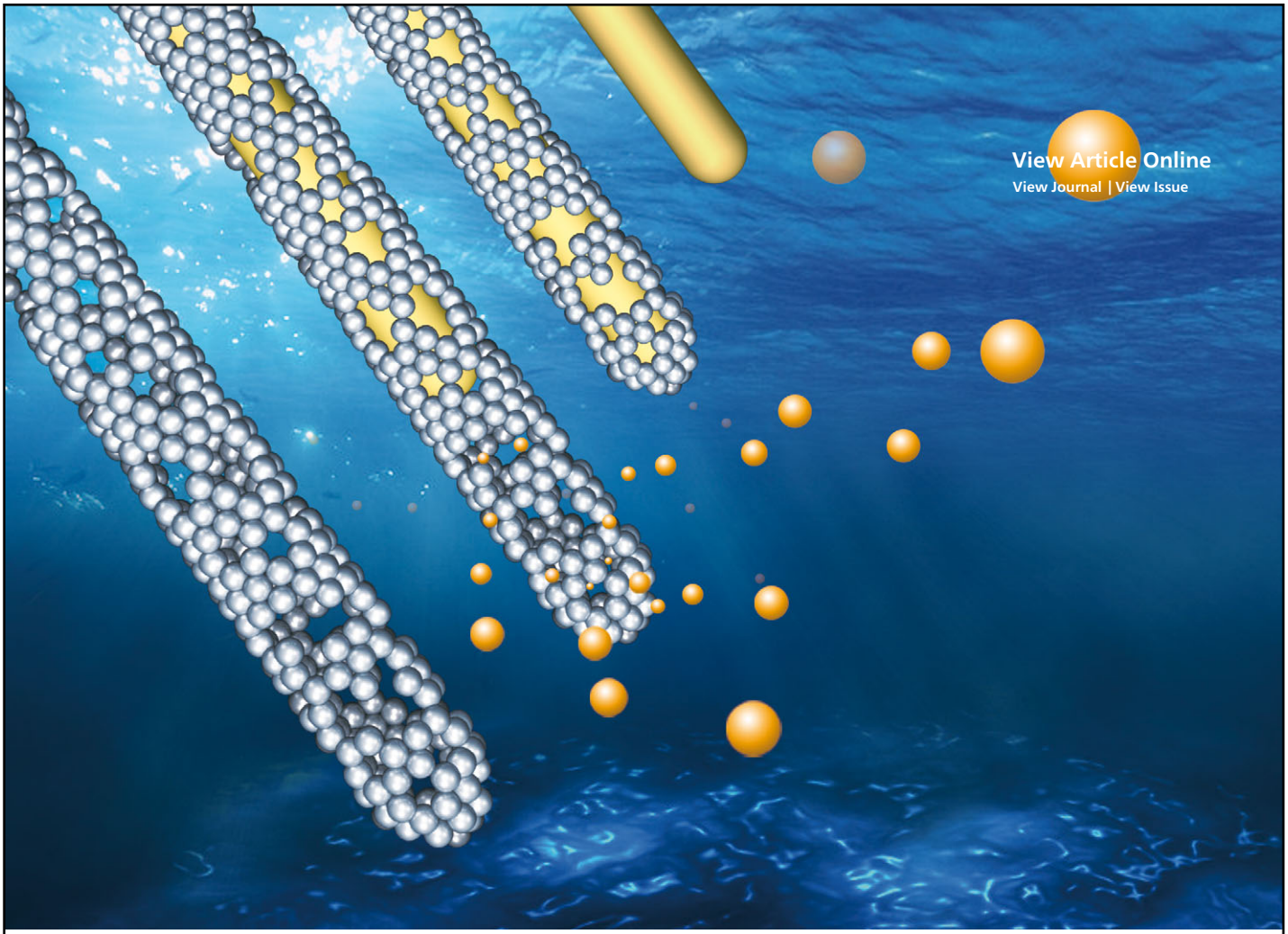

Showcasing research from Heyou Han Research Laboratory (Nano-Bioanalytic Laboratory), College of Science, State Key Laboratory of Agricultural Microbiology, Huazhong Agricultural University, China

Aqueous synthesis of porous platinum nanotubes at room temperature and their intrinsic peroxidase-like activity

PtNTs with high porosity were constructed by sacrificing the external of TeNWs and disintegrating the inner part spontaneously in aqueous solution at room temperature, which exhibited intrinsic peroxidase-like activity.

As featured in:

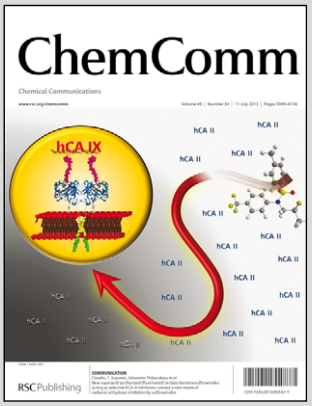

See Heyou Han *et al.*, *Chem. Commun.*, 2013, **49**, 6024.

ChemComm

RSC Publishing

COMMUNICATION

Aqueous synthesis of porous platinum nanotubes at room temperature and their intrinsic peroxidase-like activity†

Cite this: *Chem. Commun.*, 2013, **49**, 6024

Received 13th March 2013,
Accepted 8th April 2013

DOI: 10.1039/c3cc41880d

www.rsc.org/chemcomm

Kai Cai, Zhicheng Lv, Kun Chen, Liang Huang, Jing Wang, Feng Shao, Yanjun Wang and Heyou Han*

Platinum nanotubes (PtNTs) exhibiting high porosity were constructed by sacrificing the exterior of tellurium nanowires (TeNWs) and disintegrating the inner part spontaneously in aqueous solution at room temperature, in which the Kirkendall effect may play an important role. The present PtNTs exhibited intrinsic peroxidase-like activity in the presence of H_2O_2.

Platinum nanostructures such as nanoparticles, nanowires and nanotubes have attracted extensive research attention and the designs of novel platinum nanomaterials with unique properties have received considerable interest over the past several decades.[1,2] In particular, PtNTs were widely studied because of their enhanced catalytic activity, resistance to aggregation, reduced density, and unique electronic features in various application fields, such as catalysis, fuel cells, electrochemistry and biosensors.[3,4]

Porous PtNTs have more advantages than nonporous ones, especially the larger specific surface area and the porous structure which may facilitate the circulation of the reactant and reaction products.[5a] Because of the extremely high surface energies, nearly all the proposed protocols for the preparation of PtNTs, either porous or nonporous, adopted the method of template-directed synthesis. Currently available templates for obtaining PtNTs include inorganic nanowires templates,[5,6] organic templates,[4,7] viral template[8] and porous matrix templates.[9] Among them, the silver nanowire (AgNW) templates seem to be more effective in producing porous PtNTs, which were obtained through a galvanic replacement reaction of AgNWs at reflux temperature.[5a] However, AgNWs were air unstable and required inert gas protection in their own preparation and template-directed synthesis of PtNTs. Alternatively, TeNWs serve as promising templates for constructing metal nanotubes since they have the beneficial properties of high reactivity and long-term air stability and are easy to produce because trigonal tellurium has a highly anisotropic crystal structure consisting of helical chains of covalently bound atoms.[10a] Recently, ultrathin TeNWs were used as both reducing agents and sacrificial templates to synthesize PtNTs in ethylene glycol (EG) which had a high viscosity to reduce the reaction rate.[6] When EG was replaced by water, only Pt nanoparticles (NPs) could be obtained.[6,11] Notably, the shell of the PtNTs was continuous and complete rather than porous. Therefore, it is highly desirable to prepare porous PtNTs with enhanced specific surface area using air stable TeNWs as templates.

In this work, we demonstrated the synthesis of hollow platinum nanotubes with a porous shell using TeNWs as templates directly in aqueous solution at room temperature. The procedure for constructing PtNTs is shown in Fig. 1A. First, the TeNWs were synthesized by reducing tellurium dioxide with hydrazine at room temperature. Then Pt atoms were deposited *in situ* on the surface of TeNWs to form discrete Pt nanocrystals rather than a complete metallic shell with the aid of the surfactant. Finally, the inner content of elemental Te in the Te@Pt core–shell structure disintegrated and diffused spontaneously until its complete disappearance. The intrinsic peroxidase-like activity of the novel platinum nanostructure was also demonstrated.

Transmission electron microscope (TEM, Fig. 1B–D) images indicate different preparation stages: the templates (TeNWs), the intermediate products (Te@Pt core–shell nanostructures) and the final products (porous PtNTs). Their average diameter

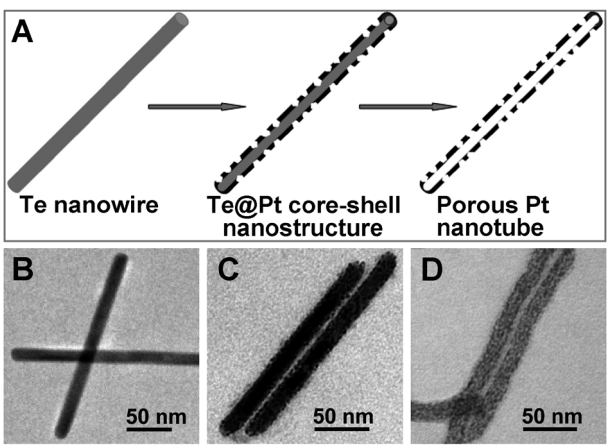

Fig. 1 (A) Schematic illustration of the evolution from Te nanowires to porous Pt nanotubes. TEM image of Te nanowires (B), Te@Pt core–shell nanostructures (C), and porous Pt nanotubes (D).

State Key Laboratory of Agricultural Microbiology, College of Science, Huazhong Agricultural University, Wuhan 430070, China. E-mail: hyhan@mail.hzau.edu.cn; Fax: +86-27-87288246; Tel: +86-27-87288246

† Electronic supplementary information (ESI) available. See DOI: 10.1039/c3cc41880d

and length are about 15 nm and 220 nm, respectively. The X-ray diffraction (XRD) pattern (Fig. S1, ESI†) shows broad peaks for the (111), (200), (220), and (311) lattice planes of the final products, which reveals that they comprised face-centered cubic (fcc) Pt crystals; and the lattice constant is about 0.39 nm, which corresponds to the standard literature values (JCPDS no. 04-0802). The broadness of these peaks indicates the nanoscale structural features of the products. A typical TEM image of the final product (Fig. 2A) shows that a number of PtNTs were produced. The hollow nanostructure and the holes in the shell of the nanotubes can be clearly observed in an enlarged magnification (Fig. 2B). The high-resolution transmission electron microscope (HRTEM, Fig. 2C) image reveals that the nanotube consists of tiny nanocrystals and an adjacent lattice fringe is approximately 0.23 nm, which corresponds to the interplanar spacing of the (111) lattice plane in the (fcc) Pt crystals. The energy-dispersive X-ray spectroscopy (EDS) analysis performed on the nanotubes in Fig. 2A (Fig. S2, ESI†) shows that Pt was the dominant element and Te was rarely present. The Te can be cleared away completely by washing and the residual elemental Te indicates that the TeNWs served as templates.

In order to understand the formation mechanism of the tubular structure, further exploration was carried out. The HRTEM image of the intermediate product (Fig. 2D) reveals that gaps already apparently existed in the shell, and the inner part of the composite structure retains the elemental Te instead of metal telluride, since the interplanar spacings of 0.59 and 0.32 nm correspond to the (001) and (101) lattice planes of trigonal tellurium (t-Te) nanowires. In addition, the transformation process from the intermediate products to the final was monitored. A series of time-dependent UV-Vis absorption spectra recorded from this process are depicted in Fig. S3 (ESI†). The absorption peak at 600–660 nm which is attributed to the length of TeNWs weakens gradually in absorbance accompanied by an obvious blue shift.[10b] This change indicates that the length of the residual TeNWs was decreasing and the structure of nanowires was disappearing. Although the transformation process took place spontaneously at room temperature, it could be accelerated by providing energy such as heating or ultrasonication.

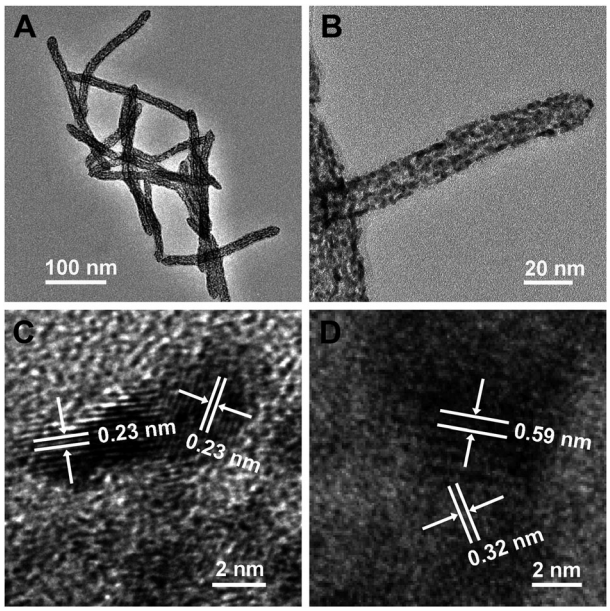

Fig. 2 (A–B) TEM images of Pt nanotubes (PtNTs), (C) HRTEM image of PtNTs, (D) HRTEM image of Te@Pt core–shell nanostructure.

The above analysis indicates that the outer part of the Te nanowires serves as a sacrificial template which is oxidized to soluble TeO_3^{2-} during the replacement reaction (eqn (1)),[6] while the inner part serves only as a physical template on which the as-reduced atomic Pt is deposited to form nanocrystals. After the formation of the Te@Pt core–shell nanostructure, the core disintegrated and diffused spontaneously to form hollow nanotubes. The Kirkendall effect, a nonequilibrium mutual diffusion process, might play an important role in the formation of the hollow Pt nanostructure at the beginning, while the later stage may be induced by another mechanism, because a large number of gaps have already formed on the surface of the intermediate products and thereby surface diffusion along the gaps or a direct elapse of residual TeNWs could take place.[12]

$$PtCl_6^{2-} + Te + 3H_2O \rightarrow Pt + TeO_3^{2-} + 6Cl^- + 6H^+ \quad (1)$$

Owing to the high reaction rate (eqn (1)), only Pt NPs with 20–60 nm in size can be obtained when water is used as solvent.[6,11] In order to slow down the reaction rate, a cationic surfactant, cetyltrimethylammonium bromide (CTAB), was chosen as a capping agent to protect TeNWs in our strategy. Moreover, CTAB might play an important role as the structure-directing agent in the formation of the incomplete shell structure.[13] In addition, the molar ratio of Pt to Te atoms in the current method is about 1 : 5, although their reaction ratio is 1 : 1. The smaller ratio allows the inner part of TeNWs to be retained and therefore it only serves as a physical template, which is important in retaining the one-dimensional (1D) nanostructure.

Biosensing based on enzyme-like nanomaterials has gradually become one of the hot topics in recent years because artificial enzymes have obvious advantages over the natural ones, such as easier preparation and higher stability.[14] Recently, Pt nanomaterials were reported to exhibit intrinsic peroxidase-like activity and have potential application in biocatalysis.[15] Herein, we evaluated the catalytic properties of the present PtNTs for catalyzing the reaction of peroxidase substrate 3,3′,5,5′-tetramethylbenzidine (TMB) to produce a blue colour reaction in the presence of H_2O_2 (Fig. 3).

The catalytic activity of the PtNTs, like natural enzymes, is dependent on pH and temperature (Fig. S4, ESI†). The optimal pH and temperature were approximately 4.0 and 20 °C, which were adopted as the standard conditions for the subsequent analysis of PtNT activity in this work. And similar to the catalyzed reaction of any natural enzyme, the PtNT catalytic reaction was inhibited at high H_2O_2 concentration (Fig. S5A, ESI†). The time-dependent absorbance was also observed (Fig. S5B, ESI†). When the concentration of H_2O_2 reached 0.5 M, the absorbance of the solution decreased slowly after 5 min, and the decrease became more obvious when the concentration was 1.0 M.

We further analyzed the peroxidase-like catalytic property of the PtNTs using steady-state kinetics. A series of kinetic data were obtained and applied to the double reciprocal of the Michaelis–Menten equation, $1/v = K_m/V_{max}\cdot(1/[S] + 1/K_m)$, where v is the initial velocity, [S] is the concentration of the substrate, K_m is the Michaelis constant and V_{max} is the maximal reaction velocity. The K_m and V_{max} were obtained using Lineweaver–Burk plots (Fig. S6, ESI†). It is observed that the oxidation reaction catalyzed by the

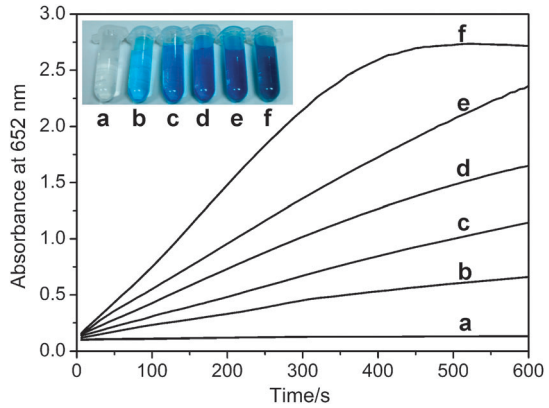

Fig. 3 The absorbance evolution at 652 nm over time at several PtNT concentrations: (a) 0 μg mL^{-1}, (b) 0.2 μg mL^{-1}, (c) 0.4 μg mL^{-1}, (d) 0.6 μg mL^{-1}, (e) 0.8 μg mL^{-1}, (f) 1.0 μg mL^{-1}. The inset shows the colour change of different samples.

PtNTs follows the typical Michaelis–Menten behavior towards the two substrates, TMB and H_2O_2.

K_m is an important parameter for measuring binding affinity of the enzyme to the substrates[16] and affects the value of the reaction rate, which is reflected intuitively in the Michaelis–Menten equation, $v = V_{max}\cdot([S]/K_m + [S])$. The apparent K_m value with TMB as the substrate under the optimum conditions for the natural enzyme horseradish peroxidase (HRP) is around 0.062 mM,[17a] while the value of the PtNTs in our work is only 0.0186 mM. The K_m value of the PtNTs which was lower than one-third of that of HRP suggests that the PtNTs had a higher affinity to TMB than HRP. Additionally, the V_{max} of the PtNTs with TMB as the substrate is three times larger than that of HRP, which is in favor of a higher reaction rate. In comparison with other nanoparticles exhibiting peroxidase-like activity in previously published reports,[17] the present PtNTs possess remarkable advantages as indicated by K_m and V_{max} (Table 1). In addition, the apparent K_m of the PtNTs with H_2O_2 as the substrate is around 155 mM, which is nearly equal to that of Fe_3O_4 MNPs; but the V_{max} of the PtNTs with H_2O_2 as the substrate is larger than those of most other nanomaterials, including Fe_3O_4 MNPs (Table S1, ESI†).

To the best of our knowledge, with TMB as the peroxidase substrate in the presence of H_2O_2, no enzyme was found to have a better effect than the present PtNTs on the two constants (K_m and V_{max}) at the same time to date. Besides the large specific surface area, the porous structure of the PtNTs may facilitate the circulation of TMB and contributes to the colour reaction. And similar to carbon nanotubes, the PtNTs have an anisotropic morphology that can improve mass transport, which may be beneficial to the reaction.[5c]

Table 1 Comparison of the kinetic parameters of different nanomaterials and HRP (TMB as a substrate). K_m is the Michaelis constant, V_{max} is the maximal reaction rate

	K_m [mM]	V_{max} [M s^{-1}]
HRP[17a]	0.062	3.61×10^{-8}
$ZnFe_2O_4$ MNPs[17b]	0.85	13.31×10^{-8}
Fe_3O_4 MNPs[17f]	0.098	3.44×10^{-8}
$Pt_{48}Pd_{52}$–Fe_3O_4 dumbbell[17a]	0.079	9.36×10^{-8}
C-Dots[17c]	0.039	3.61×10^{-8}
Co_3O_4 NPs[17d]	0.037	6.27×10^{-8}
GO–COOH[17e]	0.0237	3.45×10^{-8}
PtNTs	0.0186	11.79×10^{-8}

In summary, we have developed a facile and green method to synthesize porous PtNTs using TeNWs as templates and the result obtained indicates that the present PtNTs exhibit an intrinsic peroxidase-like activity. And the strategy of using and removing templates in this work may be applicable to other desired hollow nanostructures. Since platinum is a precious metal, the 1D hollow nanostructure with a porous surface can decrease platinum consumption effectively *via* an increase in the specific surface area in its various traditional application fields. Moreover, the unique Pt nanostructure may also find wide use as a peroxidase mimetic in biotechnology and immunoassay.

We gratefully acknowledge the funding support for this research from the National Natural Science Foundation of China (21175051), the Fundamental Research Funds for the Central Universities (2011PY139) and the Natural Science Foundation of Hubei Province Innovation Team (2011CDA115).

Notes and references

1 A. Chen and P. Holt-Hindle, *Chem. Rev.*, 2010, **110**, 3767.
2 S. Guo and E. Wang, *Nano Today*, 2011, **6**, 240.
3 Z. Peng and H. Yang, *Nano Today*, 2009, **4**, 143.
4 F. Bai, Z. Sun, H. Wu, R. E. Haddad, X. Xiao and H. Fan, *Nano Lett.*, 2011, **11**, 3759.
5 (*a*) S. M. Alia, G. Zhang, D. Kisailus, D. Li, S. Gu, K. Jensen and Y. Yan, *Adv. Funct. Mater.*, 2010, **20**, 3742; (*b*) Y. W. Lee, M. A. Lim, S. W. Kang, I. Park and S. W. Han, *Chem. Commun.*, 2011, **47**, 6299; (*c*) Z. Chen, M. Waje, W. Li and Y. Yan, *Angew. Chem., Int. Ed.*, 2007, **46**, 4060; (*d*) S. Ci, J. Zou, G. Zeng, S. Luo and Z. Wen, *J. Mater. Chem.*, 2012, **22**, 16732; (*e*) B. Mayers, X. Jiang, D. Sunderland, B. Cattle and Y. Xia, *J. Am. Chem. Soc.*, 2003, **125**, 13364.
6 H.-W. Liang, S. Liu, J.-Y. Gong, S.-B. Wang, L. Wang and S.-H. Yu, *Adv. Mater.*, 2009, **21**, 1850.
7 T. Kijima, T. Yoshimura, M. Uota, T. Ikeda, D. Fujikawa, S. Mouri and S. Uoyama, *Angew. Chem., Int. Ed.*, 2004, **43**, 228.
8 M. Ł. Górzny, A. S. Walton and S. D. Evans, *Adv. Funct. Mater.*, 2010, **20**, 1295.
9 (*a*) J. H. Yuan, K. Wang and X. H. Xia, *Adv. Funct. Mater.*, 2005, **15**, 803; (*b*) C. Chen, J. Loo, M. Deng, R. Kox, R. Huys, C. Bartic, G. Maes and G. Borghs, *J. Phys. Chem. C*, 2009, **113**, 5472.
10 (*a*) J.-M. Song, Y.-Z. Lin, Y.-J. Zhan, Y.-C. Tian, G. Liu and S.-H. Yu, *Cryst. Growth Des.*, 2008, **8**, 1902; (*b*) Z.-H. Lin, Z. Yang and H.-T. Chang, *Cryst. Growth Des.*, 2007, **8**, 351.
11 C. Zhu, S. Guo and S. Dong, *Adv. Mater.*, 2012, **24**, 2326.
12 (*a*) Y. Yin, R. Rioux, C. K. Erdonmez, S. Hughes, G. A. Somorjai and A. P. Alivisatos, *Science*, 2004, **304**, 711; (*b*) H. J. Fan, U. Gösele and M. Zacharias, *Small*, 2007, **3**, 1660; (*c*) H.-W. Liang, S. Liu and S.-H. Yu, *Adv. Mater.*, 2010, **22**, 3925.
13 (*a*) Y. Song, R. M. Garcia, R. M. Dorin, H. Wang, Y. Qiu, E. N. Coker, W. A. Steen, J. E. Miller and J. A. Shelnutt, *Nano Lett.*, 2007, **7**, 3650; (*b*) B. Y. Xia, W. T. Ng, H. B. Wu, X. Wang and X. W. Lou, *Angew. Chem., Int. Ed.*, 2012, **51**, 7213.
14 Y. Song, W. Wei and X. Qu, *Adv. Mater.*, 2011, **23**, 4215.
15 (*a*) W. He, Y. Liu, J. Yuan, J.-J. Yin, X. Wu, X. Hu, K. Zhang, J. Liu, C. Chen, Y. Ji and Y. Guo, *Biomaterials*, 2011, **32**, 1139; (*b*) J. Liu, X. Hu, S. Hou, T. Wen, W. Liu, X. Zhu, J.-J. Yin and X. Wu, *Sens. Actuators, B*, 2012, **166**, 708; (*c*) M. Ma, Y. Zhang and N. Gu, *Colloids Surf., A*, 2011, **373**, 6.
16 L. Michaelis and M. I. Menton, *Biochem. Z.*, 1913, **49**, 333.
17 (*a*) X. Sun, S. Guo, C.-S. Chung, W. Zhu and S. Sun, *Adv. Mater.*, 2012, **25**, 132; (*b*) L. Su, J. Feng, X. Zhou, C. Ren, H. Li and X. Chen, *Anal. Chem.*, 2012, **84**, 5753; (*c*) W. Shi, Q. Wang, Y. Long, Z. Cheng, S. Chen, H. Zheng and Y. Huang, *Chem. Commun.*, 2011, **47**, 6695; (*d*) J. Mu, Y. Wang, M. Zhao and L. Zhang, *Chem. Commun.*, 2012, **48**, 2540; (*e*) Y. Song, K. Qu, C. Zhao, J. Ren and X. Qu, *Adv. Mater.*, 2010, **22**, 2206; (*f*) L. Gao, J. Zhuang, L. Nie, J. Zhang, Y. Zhang, N. Gu, T. Wang, J. Feng, D. Yang, S. Perrett and X. Yan, *Nat. Nanotechnol.*, 2007, **2**, 577.

